A study on computer-aided design of PIN-diode phase modulators at microwave frequencies

Schjær-Jacobsen, Hans

Publication date:
1976

Document Version
Publisher's PDF, also known as Version of record

A STUDY ON

COMPUTER-AIDED DESIGN OF PIN-DIODE PHASE MODULATORS AT MICROWAVE FREQUENCIES

BY

HANS SCHJÆR-JACOBSEN

JULY 1976

LIST OF CONTENTS

FOREWORD

This report describes some preliminary investigations and attempts in connection with computer-aided design of PIN diode phase modulators for usage at microwave frequencies in the K_u-band.

The study has been carried out from August 1, 1975 to July 31, 1976 while I was affiliated with Institut für Hochfrequenztechnik, Technische Universität Braunschweig, Federal Republic of Germany. Professor Dr. H.-G. Unger is acknowledged for his encouragement to undertake this study. The Alexander von Humboldt Stiftung, Bonn-Bad Godesberg and the Danish Council for Technical and Scientific Research, Copenhagen are acknowledged for financially supporting my stay in Germany.

Several members of the staff at Institut für Hochfrequenztechnik have contributed to my understanding of phase modulators, in particular Dr. Schünemann and Mr. Begemann. For this I owe them many thanks.

Braunschweig, July 1976

Hans Schjær-Jacobsen

1. INTRODUCTION

The reflection-type phase modulator may be considered a vital component in modern microwave PCM communication links. The ideal operating condition for this component is achieved when it switches abrubtly between two static states, giving rise to reflection coefficients of unit amplitude and a specific phase difference, both maintained over a certain frequency band of interest. In practice, unit amplitude is not reached because of inherent losses in the active switching element (f.ex. a PIN diode) and the embedding network. It may even be difficult to achieve equal amplitudes. Moreover, the phase difference between the two static states of operation is usually very frequency sensitive. This means that a non-ideal phase modulator may be characterized by the phase error

$$\varepsilon = \phi_0 - \phi \ ,$$

the amplitude imbalance

$$\Delta = |\rho_2/\rho_1| \ ,$$

and, in cases of balanced amplitudes, the insertion loss

$$L = 20 \log_{10}|\rho| \ .$$

Here ϕ_0 is the specified phase difference, ϕ the actual phase difference between the reflection coefficients ρ_1 and ρ_2 in the two states, and $|\rho| = |\rho_1| = |\rho_2|$. Note that the three characteristic numbers ε, Δ, and L are functions of the frequency.

The purpose of this study is to try to make use of a computer-aided design technique in order to optimize the performance of the modulator over a specified frequency band. To this end it is nescessary to develop a computer model of the modulator which enables us to analyze its performance over the frequency band of interest. At an early

stage of the study it was decided to build the modulator at K_u-band (12.4 - 18.0 GHz) and to use sections of ridge waveguides as transition between the PIN diode as switching element and a rectangular waveguide. In the next few sections we shall therefor consider in some more detail the analysis of ridge waveguides and the design of such broadband transitions.

2. ANALYSIS OF RIDGE WAVEGUIDES

2.1 Theory

The cross-sectional shape of ridge waveguides is shown in Fig. 1. The theoretical analysis of this modification of rectangular waveguides has been the subject of several papers during the last years. Cohn [1] calculated the cutoff wavelength and characteristic impedance of ridge waveguides. His impedance calculations were based on the current-voltage definition and the discontinuity capacitances at the edge of the ridge were neglected. See also [2]. Mihran [3] extended the impedance calculations to include the discontinuity capacitances and also presented a formula for the impedance based on the power-voltage definition. Unger [4] considered ridge waveguides with cross-sections not covered by the previously developed formulas and Hopfer [5] presented formulas for the attenuation and power handling capacity. In the paper by Pyle [6] tabulated data of the cutoff wavelengths may be found as well as correction curves for extension of the data to other aspect ratios.

In our study we shall consider a single ridge waveguide. In order to calculate the cutoff wavelength λ_c for the TE_{10} mode we have to solve the transverse resonance equation for λ_c taking into account the susceptance created by the discontinuity step in the tranverse direction. The equation is

$$\frac{b_1}{b_2} \operatorname{tg}\left(\pi \frac{a_2}{\lambda_c}\right) + \frac{B}{Y_0} - \cot\left(\pi \frac{a_1 - a_2}{\lambda_c}\right) = 0 , \qquad (1)$$

where a_1, a_2, b_1, and b_2 are defined in Fig. 1. The normalized step

susceptance B/Y_0 is itself a function of λ_c and is calculated according to formulas given in [7]. Thus (1) becomes a fairly complicated transcendental equation which has to be solved by iterative numerical methods.

Having determined λ_c we make use of a power-voltage impedance definition [3] to calculate the impedance Z_{pv}^{∞} at infinit frequency

$$Z_{pv}^{\infty} = \frac{120\pi^2 b_2/\lambda_c}{\frac{b_2}{b_1}\frac{B}{Y_0}\cos^2\theta_2 + \frac{\theta_2}{2} + \frac{\sin 2\theta_2}{4} + \frac{b_2}{b_1}\frac{\cos^2\theta_2}{\sin^2\theta_1}\left[\frac{\theta_1}{2} + \frac{\sin 2\theta_1}{4}\right]}, \quad (2)$$

where

$$\theta_1 = \pi\frac{a_1 - a_2}{\lambda_c}, \quad \theta_2 = \pi\frac{a_2}{\lambda_c}. \quad (3)$$

The impedance at any frequency may then be found by

$$Z_{pv} = \frac{Z_{pv}^{\infty}}{\sqrt{1 - (\frac{\lambda}{\lambda_c})^2}}. \quad (4)$$

2.2 Computer Implementation

To solve the transcendental equation (1) for λ_c we use the well known regula-falsi iteration technique. Thereby two initial estimates of λ_c have to be guessed and afterwards the iterations are carried out to a specified accuracy. This has been implemented in FORTRAN subroutine RIDGE1 which also calculates the impedance. In addition, the subroutine STEPB for calculation of the step susceptance B/Y_0 must be supplied. Also the ideal case where the step susceptance is neglected has been programmed. In this case the Newton-Raphson iteration technique was used, the analysis being implemented in the subroutine RIDGEI. Thus, the cutoff wavelength and impedance may be calculated for (almost) arbitrary geometry of the ridge waveguide.

2.3 Computed Results

In Figs. 2 and 3 computed results are shown for the normalized TE_{10} cutoff wavelength λ_c/a_1 and the impedance Z_{pv}^{∞} as a function of a_2/a_1. Parameter for the curves is b_2/b_1 and b_1/a_1 is fixed to 0.5, a value which is chosen because it corresponds to the dimensions of the rectangular waveguide used later on.

Although not quoted here, results have also been computed when the step susceptance in the transverse plane is neglected. As expected, these results differ considerably from those of Figs. 2 and 3. Consequently, it is justified to take this susceptance into account.

3. CASCADED SECTIONS OF RIDGE WAVEGUIDES

3.1 Scattering Matrices

When several sections of ridge waveguides with different heights of the ridge (the geometrical dimension b_2) are cascaded, we shall analyze the frequency performance by means of scattering parameters. Thereby each section of ridge waveguide is considered to be a twoport with scattering matrix $\underline{\underline{S}}$ and real normalizing impedances r_1 and r_2. The junction between two sections of waveguides is also considered a twoport.

Generally, we have the scattering matrix for a piece of lossy transmission line with characteristic impedance Z_0, complex propagation constant γ, and physical length ℓ

$$\underline{\underline{S}} = \frac{1}{Z_0^2 + Z_0(r_1+r_2)\coth(\gamma\ell) + r_1 r_2} \times \begin{bmatrix} Z_0^2 + Z_0(r_2-r_1)\coth(\gamma\ell) - r_1 r_2 & 2Z_0\sqrt{r_1 r_2}\,\operatorname{csch}(\gamma\ell) \\ 2Z_0\sqrt{r_1 r_2}\,\operatorname{csch}(\gamma\ell) & Z_0^2 + Z_0(r_1-r_2)\coth(\gamma\ell) - r_1 r_2 \end{bmatrix} \tag{5}$$

where r_1 and r_2 are the normalization constants, see Fig. 4. As Z_0 we use

the impedance Z_{pv} defined by (4) for the particular section of ridge waveguide under consideration and assume the waveguide to be lossless.

The junction scattering matrix is defined for a junction with a parallel impedance Z (representing the discontinuity effect caused by the change in ridge height, see Section 3.2):

$$\underline{\underline{S}} = \frac{1}{r_1 r_2 + Z(r_1+r_2)} \begin{bmatrix} Z(r_2-r_1) - r_1 r_2 & 2Z\sqrt{r_1 r_2} \\ 2Z\sqrt{r_1 r_2} & Z(r_1-r_2) - r_1 r_2 \end{bmatrix} \qquad (6)$$

see Fig. 5.

Having calculated the scattering matrices for the chain of twoports with properly chosen normalization constants, the total scattering matrix is found by transforming each scattering matrix to its transfer scattering matrix, multiplying all the transfer scattering matrices together, and transform back to the total scattering matrix. The whole process is repeated as many times as required by the analysis.

3.2 A Note on Discontinuity Capacitances

When two ridge waveguides with different heights of the ridge, but otherwise identical dimensions, are coupled together, there will be a discontinuity in the longitudinal direction of the combined waveguide. The lack of data for this type of discontinuity may suggest that it either be neglected or it be represented by a simple model, namely that of the parallel plane discontinuity capacitance C_d by Whinnery and Jamieson [8], see Fig. 6. Both possibilities are accounted for by the introduction of the complex impedance Z in (6).

3.3 Computer Implementation

A number of subroutines have been written in order to implement these ideas. SLINEL and S2PJZ compute (5) and (6), respectively. S2TOT converts the scattering matrix of a twoport to its transfer

scattering matrix and T2TOS does the opposit conversion. C2MUL performs the multiplication of the transfer scattering matrices. The Whinnery and Jamieson formula is implemented in the subroutine CSTAT.

4. DESIGN OF BROAD-BAND RIDGE WAVEGUIDE TRANSFORMERS

4.1 Analysis of the Transformers

For the analysis of a single ridge waveguide transition inserted between a rectangular and single ridge waveguide a FORTRAN subroutine RWGTRA has been written. It analyzes the frequency dependency of the complex reflection coefficient ρ for arbitrary geometrical dimensions of the waveguides and an arbitrary number N_{sect} of transformer sections, see Fig. 7. The program is based on the ideas developed in the previous sections of this report. The subroutine parameter list with an explanation of the parameters is shown in Fig. 8.

4.2 Optimization Technique

To design broad-band ridge waveguide transformers we shall make use of the minimax optimization formulation. According to this we shall try to minimize the maximum voltage standing wave ratio (VSWR) within a specified band of frequency. Let the complex reflection coefficient sampled at the j'th sample frequency be denoted by ρ_j, $j=1,\ldots,m$. We then have for the minimax objective function to be minimized

$$F(\underline{x}) = \max_{1\leq j\leq m} \left| \frac{1 + |\rho_j(\underline{x})|}{1 - |\rho_j(\underline{x})|} \right| \qquad (7)$$

where the vector $\underline{x}$ contains the n optimization parameters, $m > n$, f.ex. the geometrical dimensions of the transformer for a given number of sections. We apply the non-linear minimax optimization method reported in [9] to minimize (7). A description of the optimization program MINI2W is given in [10]. It requires a subroutine to be written for evaluation

of (7) which we of course do by the help of subroutine RWGTRA. This is straight forward and will not be further described in this report. A special version of MINI2W was developed to be used with the ICL computers at the Rechenzentrum, Technische Universität Braunschweig.

4.3 Examples

Examples of minimax optimized transformers with two sections of ridge waveguide are given in Table I and Fig. 9. The rectangular waveguide used has the dimensions a_1=15.8 mm and b_1=7.9 mm. The ridge has got a thickness of a_2=4.0 mm and the air gap dimension b_2=3.0 mm. The optimization parameters $(x_1,\ldots,x_4)$ are defined in Fig. 9 and the initial values are given in Table I. The dotted response curve in Fig. 9 corresponds to the transformer having the dimensions given by the initial parameters. Here the maximum VSWR within the frequency bands considered is 1.42. The curve marked R gives the impedance ratio of the transformer.

Three optimizations are subsequently carried out using the initial parameters as starting points, however with different frequency bands. In all cases the transformer response is sampled in intervals of 0.1 GHz. Table I gives the resulting parameter values and VSWR as well as the number of response evaluations required in order to obtain convergence to the minimax solution. The optimized responses are also shown in Fig. 9.

Three-section transformers have also been considered. In Fig. 10 two optimized responses are shown as well as the initial one. The rectangular and ridge waveguides have the same dimensions as shown in Fig. 9, however, three sections are used instead of two. Within the frequency band 12-18 GHz the maximum VSWR has been minimized to 1.03 and within the band 13-17 GHz to 1.008. Although not shown, the response curve in the latter case is equal ripple just as seen on the other responses.

5. PIN DIODE REFLECTION MODULATOR

5.1 Description of Modulator Structure

A sketch of the modulator structure under consideration is shown in Fig. 11. The PIN diode is mounted in a ridge waveguide which is short circuited in a certain distance to the right and transformed via a stepped transformer to the rectangular waveguide to the left. The The diode itself is packaged in an S4 package and switched between the two static states of operation trough a connection (not shown) in the upper waveguide wall. The stepped transformer may have an arbitrary number of steps and the ridge waveguide dimensions may also take arbitrary values, just as for the broad-band transformers previously considered in Section 4.

5.2 Representation of the Diode

The PIN diode is represented by small signal equivalent circuits, one for each of the static states of operation. In Fig. 12(a) the forward bias equivalent circuit is shown and in Fig. 12(b) the corresponding reverse bias equivalent circuit. Here C_p and L_p are the package capacitance and inductance, respectively. C_j is the junction capacitance. R_f is composed of the junction resistance and the residual resistance whereas R_r is equal to the residual resistance. For the reverse bias small signal impedance Z_2 we get

$$Z_2 = \frac{R_r + j[\omega L_p(1-\omega^2 L_p C_p + 2C_p/C_j) - (1+C_p/C_j)/(\omega C_j) - \omega C_p R_r^2]}{(1+C_p/C_j - \omega^2 L_p C_p)^2 + (\omega C_p R_r)^2}, \quad (8)$$

where ω is the angular frequency. The forward bias impedance Z_1 is easily obtained from (8) by letting $C_p \to \infty$ and substituting R_f for R_r. These formulas have been implemented in a subroutine PINIMP, which also calculates the hyperbolic middle point impedance Z_m, see the following Section.

5.3 Formulation of Design Procedure

The modulator is considered to be a loss less, linear embedding of a non-ideal two-state switching element, f.ex. a PIN diode. The embedding must simultaneously transform the two diode states so as to give input reflection coefficients with equal magnitude and specified phase difference as described in the introduction. For the case of a π modulator, which we shall consider, Navarro [11] and Dorschner [12] has shown that this may be obtained with an embedding network which matches the hyperbolic middle point impedance Z_m of the diode. Thereby the design problem is reduced to that of an impedance matching problem. $Z_m = R_m + jX_m$ is defined in terms of the diode impedances $Z_1 = R_1 + jX_1$ and $Z_2 = R_2 + jX_2$

$$R_m = \sqrt{R_1 R_2}\sqrt{1 + \left(\frac{X_1 - X_2}{R_1 + R_2}\right)^2}$$

$$X_m = \frac{R_1 X_2 + R_2 X_1}{R_1 + R_2} \quad . \tag{9}$$

Since, in our approach, we intend to design modulators that perform over a certain band width, the impedance matching problem has to be solved over this band width. Therefor we shall try to adjust the parameters of the embedding network, i.e. the geometrical dimensions of the ridge waveguide in Fig. 11, so as to minimize the maximum reflection coefficient when the embedding network is loaded with the hyperbolic middle point impedance Z_m, see Fig. 13. The analysis of the structure in Fig. 11 is carried out in a subroutine RWGMOD which is also used in connection with the minimax optimization program MINI2W as described for the broad band transformers in Section 4.

5.4 Design Example

We describe a practical design example with the PIN diode data $C_p = 0.13\ 10^{-3}$ nF, $L_p = 0.3$ nH, $R_f = 0.3$ Ohm, $R_r = 0.5$ Ohm, and $C_j = 0.15\ 10^{-3}$ nF. These data should be representative for commercial available diodes. The objective is to design a π modulator with a center frequency of 14.55 GHz and a band width of 0.2 GHz using the structure in Fig. 11, however with only one section of ridge waveguide. The parameters to be varied are $(x_1,\ldots,x_4)$ as defined in Fig. 14 where also the additional geometrical dimensions of the structure are given. The initial and optimized values of the parameters are given in Table II and the initial and optimized frequency responses of the reflection coefficient $|\rho_m|$ are shown in Fig. 15. Clearly, the hyperbolic middle point impedance has been matched in the best possible way within the frequency band of interest 14.45 - 14.65 GHz. Also the phase and amplitude errors have been calculated. The maximum phase error in the frequency band was 13 deg. whereas the absolute values of the reflection coefficients in the two static states of operation were of the order of 0.96. The amplitude imbalance was very small, $\Delta = 1.001$ approximately. The reflection coefficients and, consequently, the amplitude imbalance are nearly constant as functions of frequency. In contrast to this, the phase error is strongly dependent on the frequency, see Fig. 16. The phase error seems therefor to be the crucial factor in this design. There is probably no doubt, however, that the parameters found represent the optimal solution for the given frequency band and the given physical structure. Whether or not the resulting phase and amplitude errors are sufficiently small is a question of system considerations, which are not the subject of this report.

5.5 Preliminary Measurements

A laboratory model of the modulator designed in the previous Section was built and measurements carried out as preliminary attempts to establish a correspondence between the theoretical model and practical modulators. The experimental model was provided with some tuning facilities. The short circuit was built as a sliding short circuit which could be adjusted by means of a screw. Further two tuner screws were mounted above the steps in the ridge waveguide in order to be able to tune the step capacitances. The ridge waveguide itself was provided with an undercut to get better contact with the waveguide wall.

The measuring setup previously developed at the Institut für Hochfrequenztechnik for measuring the reflection coefficients and phases was made available. For the present modulator the theoretical results were not verified to an acceptable degree. The problem seem to be too high losses in the modulator. The reflection coefficients at the center frequency could not be measured larger than of the order of 0.7 in the two states of operation. The phase error could at the same time be tuned to zero. No measurements at other frequencies were carried out due to the excessive losses.

5.6 Discussion

The computer-aided design technique developed in this report seemes to work satisfactorily in the sense that it results in theoretical designs which are optimal in the minimax sense. There are two main problems to be discussed in connection with the work. 1) The excessive high losses in the experimental model. 2) The limited band width obtainable with the chosen structure.

1) Probably the losses are due to a bad construction of the gliding short circuit. Whereas short circuits are easily constructed in rectangular waveguides it its somewhat more difficult in ridge waveguides. The time did not permit to make further experiments with other constructions.

2) In view of the extreme broad band width obtained by the optimized transformers in Section 4 it was expected that also the modulators could be designed very broad banded. The design example in Section 5.4 does not seem to support this point of view. The question therefor arises: what are the limiting factors for the band width obtaiable? This question suggests more fundamental investigations to be carried out concerning embedding networks. In the author's opinion one of the limiting factors may be found in the short circuited piece of transmission line behind the diode. It would be interesting to investigate whether more complicated structures behind the diode would yield better results.

Finally a better method should be found for modelling of the PIN diode. In this work we have used "typical" parameter values for the equivalent circuits of the two static states of operation. It is uncertain to which degree the actual diode is represented by these data. The best way would certainly be to develop a method for measuring the small signal impedances for the particular diode, f.ex. by means of a computer controlled network analyzer.

6. REFERENCES

[1] S.B. Cohn, "Properties of ridge wave guide", Proc. IRE, Vol. 35, pp. 783-788, August 1947.

[2] N. Marcuwitz, Waveguide Handbook, M.I.T. Readiation Lab. Series, Vol. 10, pp. 399-402, New York, McGraw-Hill, 1951.

[3] T.G. Mihran, "Closed- and open-ridge waveguide", Proc. IRE, Vol. 37, pp. 640-644, June 1949.

[4] H.-G. Unger, "Die Berechnung von Steghohlleitern", A.E.U., Vol. 9, pp. 157-161, April 1955.

[5] S. Hopfer, "The design of ridged waveguides", IRE Trans. Microwave Theory Techn., Vol. MTT-3, pp. 20-29, October 1955.

[6] J.R. Pyle, "The cutoff wavelength of the TE_{10} mode in ridged rectangular waveguide of any aspect ratio", IEEE Trans. Microwave Theory Techn., Vol. MTT-14, pp. 175-183, April 1966.

[7] N. Marcuwitz, Waveguide Handbook, M.I.T. Radiation Lab. Series, Vol. 10, pp. 307-308, New York, McGraw-Hill, 1951.

[8] J.R. Whinnery and H.W. Jamieson, "Equivalent circuits for discontinuities in transmission lines", Proc. IRE, Vol. 32, pp. 98-114, February 1944.

[9] K. Madsen, O. Nielsen, H. Schjær-Jacobsen, and L. Thrane, "Efficient minimax design of networks without using derivatives", IEEE Trans. Microwave Theory Techn., Vol. MTT-23, pp. 803-809, October 1975.

[10] K. Madsen and H. Schjær-Jacobsen, "A non-linear minimax optimization program not requiring derivatives", Computer Program Description, to appear in IEEE Trans. Antennas Propagat., May 1977.

[11] M.S. Navarro, "Modulator embedding networks for PIN diodes", MIT RLE QPR No. 106, pp. 23-27, July 15, 1972.

[12] T.A. Dorschner, "Characterization of reflection phase modulators using hyperbolic geometry", Proc. European Microwave Conf., Paper No. A.9.1., Brussels, Belgium, September 4-7, 1973.

CAPTIONS FOR TABLES AND FIGURES.

Table I. Optimization of two-section ridge waveguide transformers. a_1=15.8, a_2=4.0, b_1=7.9, and b_2=3.0 mm.

Table II. Optimization of PIN diode reflection phase modulator from 14.45 to 14.65 GHz.

Fig. 1. Cross sections of ridge waveguides.

Fig. 2. Normalized TE_{10} cutoff wavelength for single ridge waveguide.

Fig. 3. Impedance at infinit frequency for single ridge waveguide.

Fig. 4. Lossy transmission line considered as a twoport.

Fig. 5. A junction between two twoports considered as a twoport.

Fig. 6. Parallel plane discontinuity capacitance [8].

Fig. 7. Ridge waveguide transformer with nsect sections.

Fig. 8. Explanation of parameters in FORTRAN subroutine RWGTRA.

Fig. 9. Optimized ridge waveguide transformers with two sections.

Fig. 10. Optimized ridge waveguide transformers with three sections.

Fig. 11. Basic modulator structure.

Fig. 12. Small signal equivalent circuits for PIN diode. (a) Forward bias. (b) Reverse bias.

Fig. 13. Hyperbolic middle point impedance matching problem.

Fig. 14. Actual modulator structure with optimization parameters $\underline{x}$. a_1=15.8, b_1=7.9, a_2=7.0, and b_2=2.0 mm.

Fig. 15. Initial and optimized frequency responses for modulator.

Fig. 16. Resulting phase error as function of frequency.

Bandwidth [GHz]	Max. VSWR	bx_1	bx_2 [mm]	ℓ_1	ℓ_2	Number of Response Evaluations
Initial:	1.42	6.330	4.670	5.750	5.450	--
12.4 - 18.0	1.10	6.108	4.057	5.789	5.305	63
13.0 - 17.0	1.05	6.164	4.019	5.858	5.352	76
14.0 - 16.0	1.01	6.207	3.987	5.819	5.313	75

Table I. Optimization of two-section ridge waveguide transformers. a_1=15.8, a_2=4.0, b_1=7.9, and b_2=3.0 mm.

[mm]	Initial	Optimized
x_1	4.52	5.79
x_2	6.17	7.10
x_3	7.93	7.61
x_4	12.0	12.97

Table II. Optimization of PIN diode reflection phase modulator from 14.45 to 14.65 GHz.

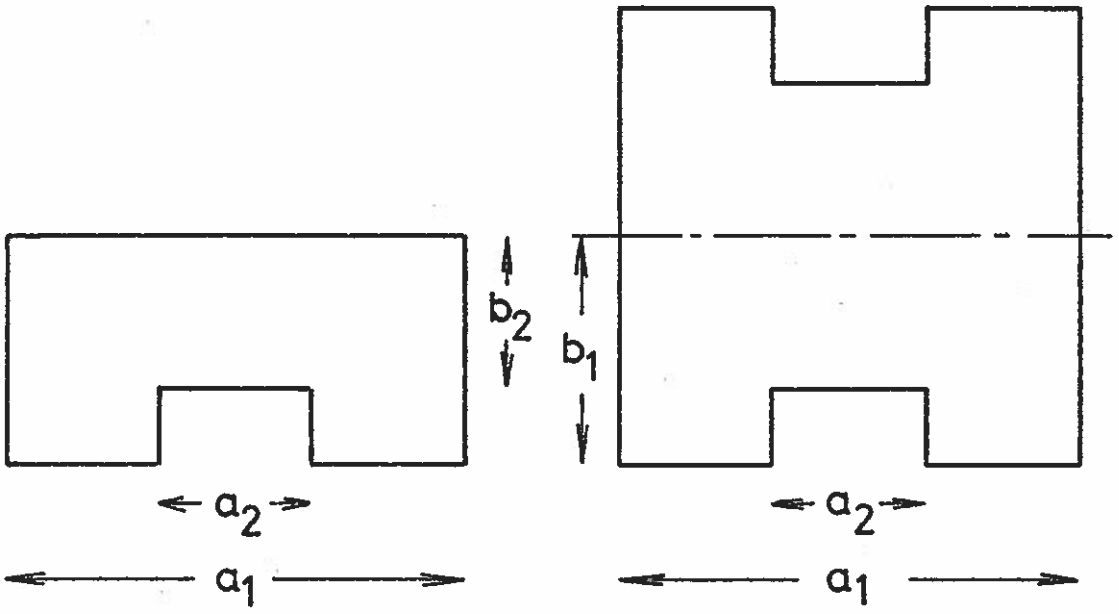

Fig. 1. Cross sections of ridge waveguides.

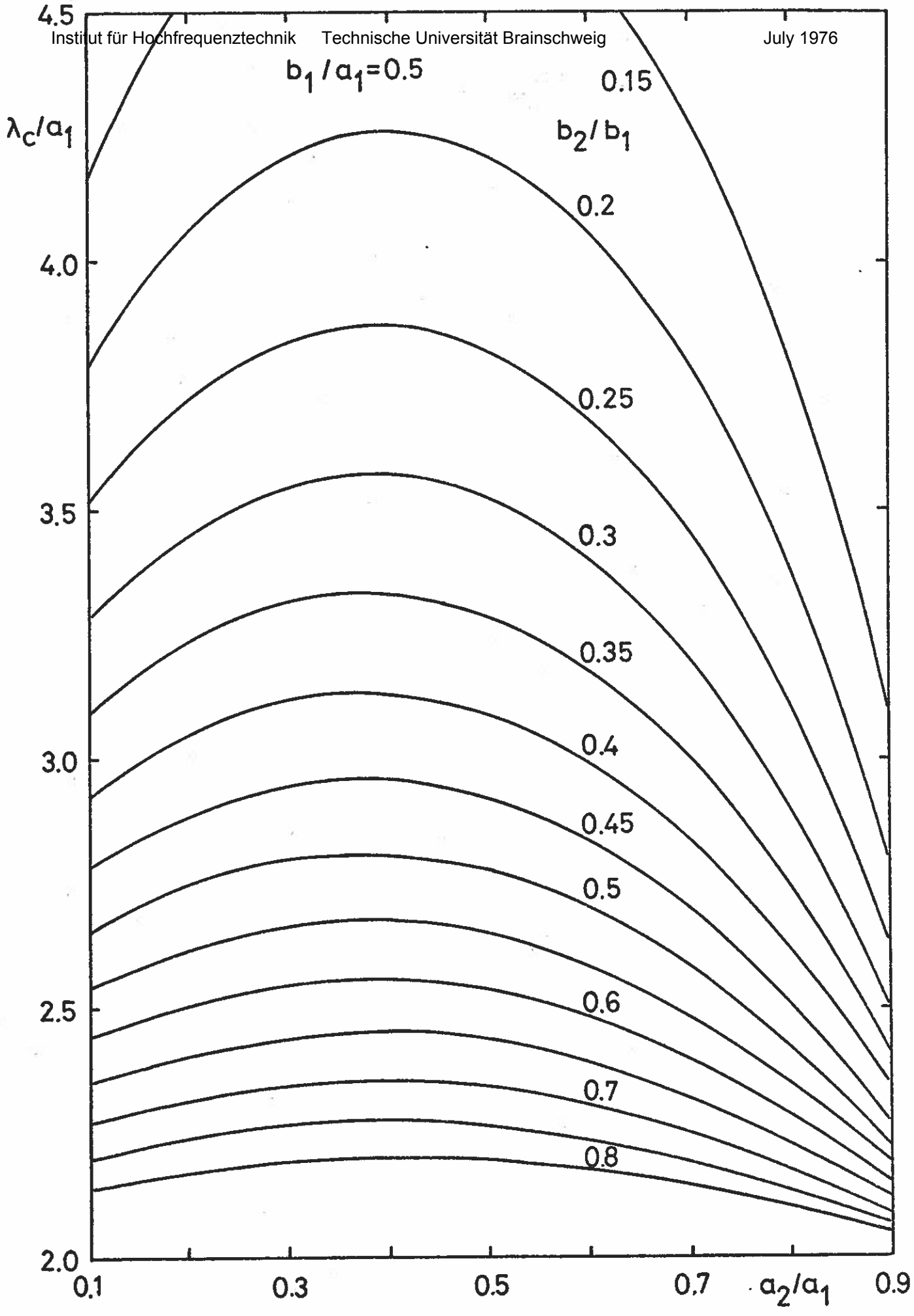

Fig. 2. Normalized TE_{10} cutoff wavelength for single ridge waveguide.

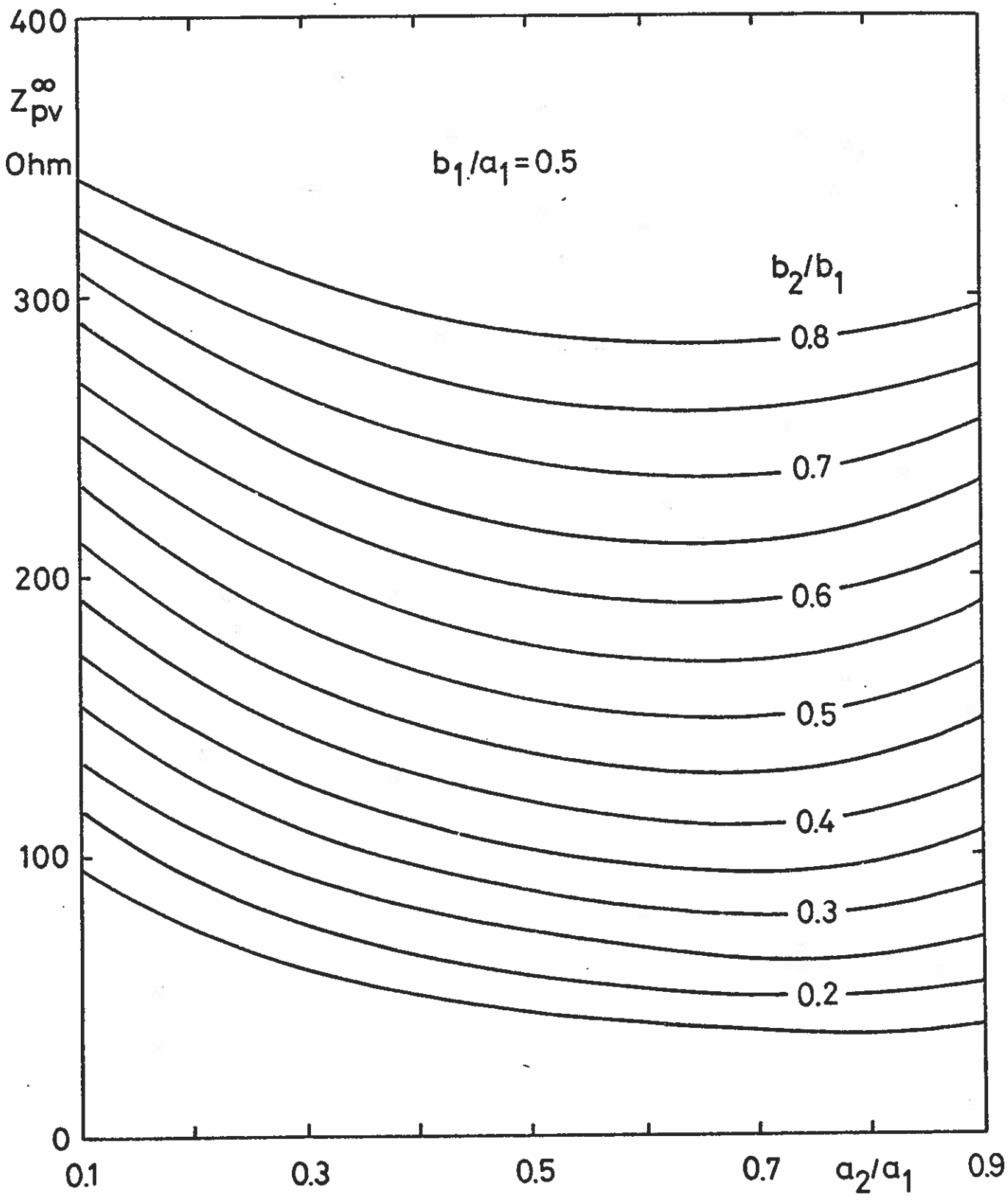

Fig. 3. Impedance at infinit frequency for single ridge waveguide.

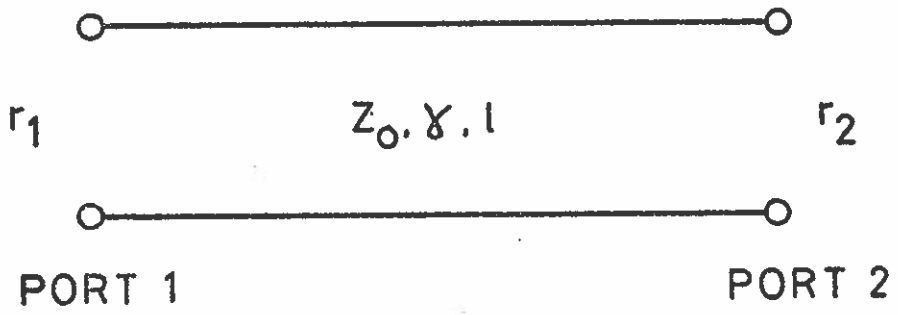

Fig. 4. Lossy transmission line considered as a twoport.

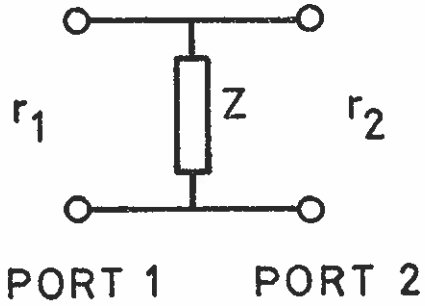

Fig. 5. A junction between two twoports considered as a twoport.

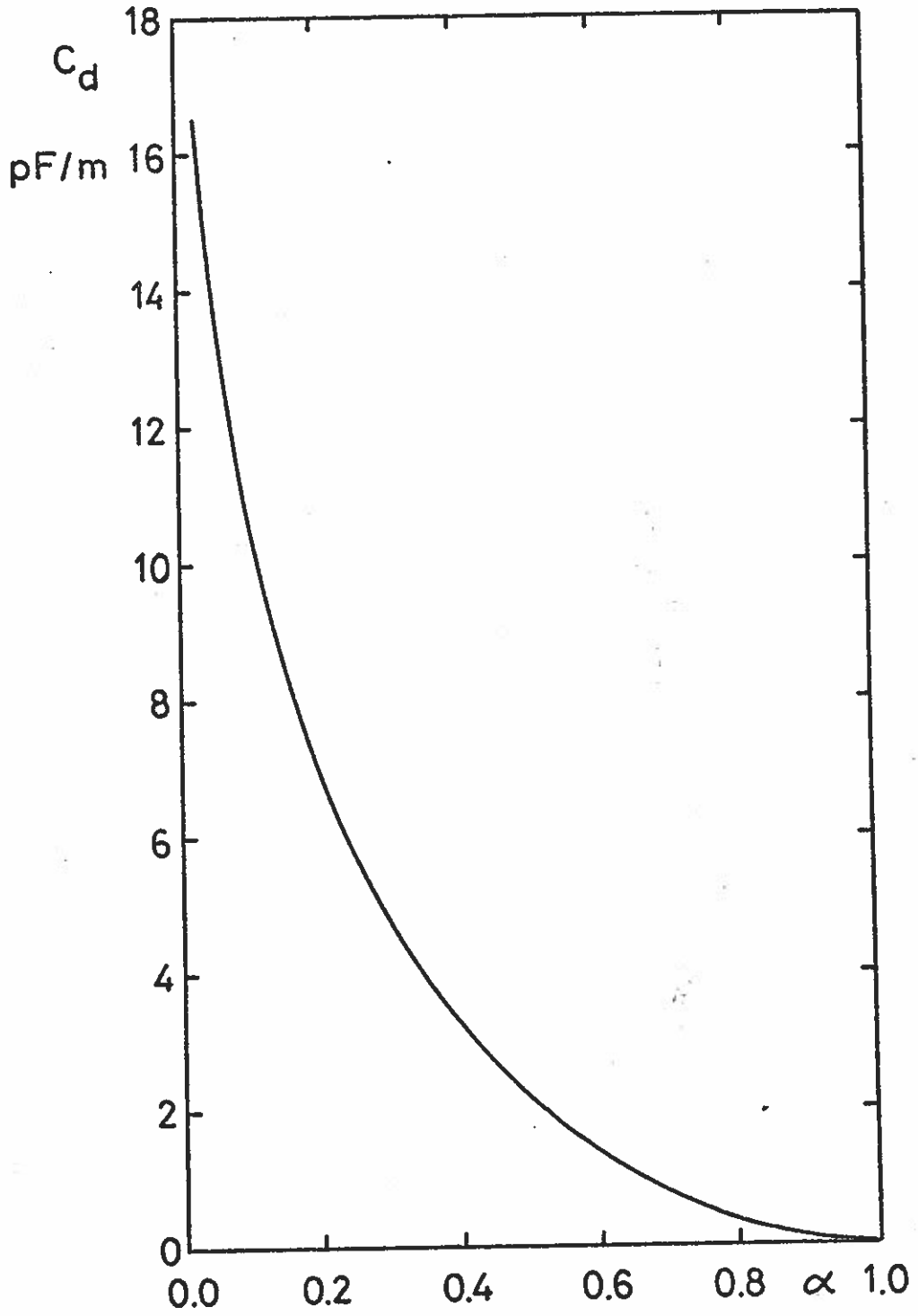

Fig. 6. Parallel plane discontinuity capacitance [8].

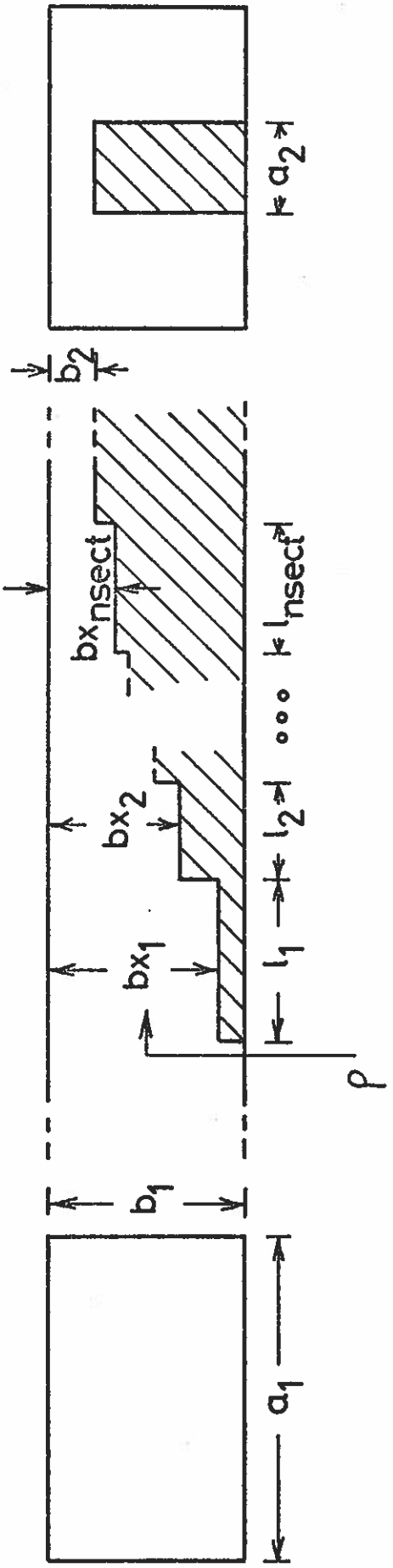

Fig. 7. Ridge waveguide transformer with nsect sections.

```
ABLISTEN
      SUBROUTINE RWGTRA(F0,NFREQ,DFREQ,NSECT,A1,B1,A2,B2,BX,ALENG,
     1                  CLAMB,ZINF,RHO)
C
C    SUBROUTINE RWGTRA CALCULATES THE COMPLEX REFLECTION COEFFICIENT
C    RHO OF A RIDGE WAVEGUIDE TRANSITION WITH NSECT SECTIONS,
C    INSERTED BETWEEN A RECTANGULAR AND A RIDGE WAVEGUIDE.
C    SUBROUTINES RIDGE1, STEP4, S2P3, S2TOT, T2TOS, SLINEL, C2MUL,
C    AND CSTAT SHOULD BE SUPPLIED.
C
C    INPUT PARAMETERS
C    F0          CENTER FREQUENCY :GHZ>.
C    NFREQ       NUMBER OF FREQUENCY POINTS, NFREQ ODD.
C    DFREQ       DISTANCE BETWEEN FREQUENCY POINTS :GHZ>.
C    NSECT       NUMBER OF SECTIONS, NSECT.GE.1.
C    A1          WIDTH OF RECTANGULAR WAVEGUIDE :MM>.
C    B1          HEIGHT OF RECTANGULAR WAVEGUIDE :MM>.
C    A2          WIDTH OF RIDGE :MM>.
C    B2          HEIGHT OF RIDGE WAVEGUIDE, AIR GAP DIMENSION :MM>,
C    BX          ARRAY OF DIMENSION NSECT CONTAINING THE HEIGHTS OF TRANS-
C                FORMER SECTIONS, AIR GAP DIMENSIONS, NUMBERED FROM RECT-
C                ANGULAR WAVEGUIDE :MM>.
C    ALENG       ARRAY OF DIMENSION NSECT CONTAINING THE LENGTHS OF TRANS-
C                FORMER SECTIONS, NUMBERED FROM RECTANGULAR WAVEGUIDE :MM>,
C
C    OUPUT PARAMETERS
C    CLAMB       ARRAY OF DIMENSION NSECT CONTAINING CUT-OFF WAVELENGTHS
C                OF TRANSFORMER SECTIONS :MM>.
C    ZINF        ARRAY OF DIMENSION NSECT CONTAINING CHARACTERISTIC
C                IMPEDANCES OF TRANSFORMER SECTIONS AT INFINIT
C                FREQUENCY, POWER-VOLTAGE DEFINITION :OHM>.
C    RHO         COMPLEX ARRAY OF DIMENSION NFREQ CONTAINING COMPLEX
C                REFLECTION COEFFICIENT.
C
C    DECEMBER 1975, HS-J.
C
```

Fig. 8. Explanation of parameters in FORTRAN subroutine RWGTRA.

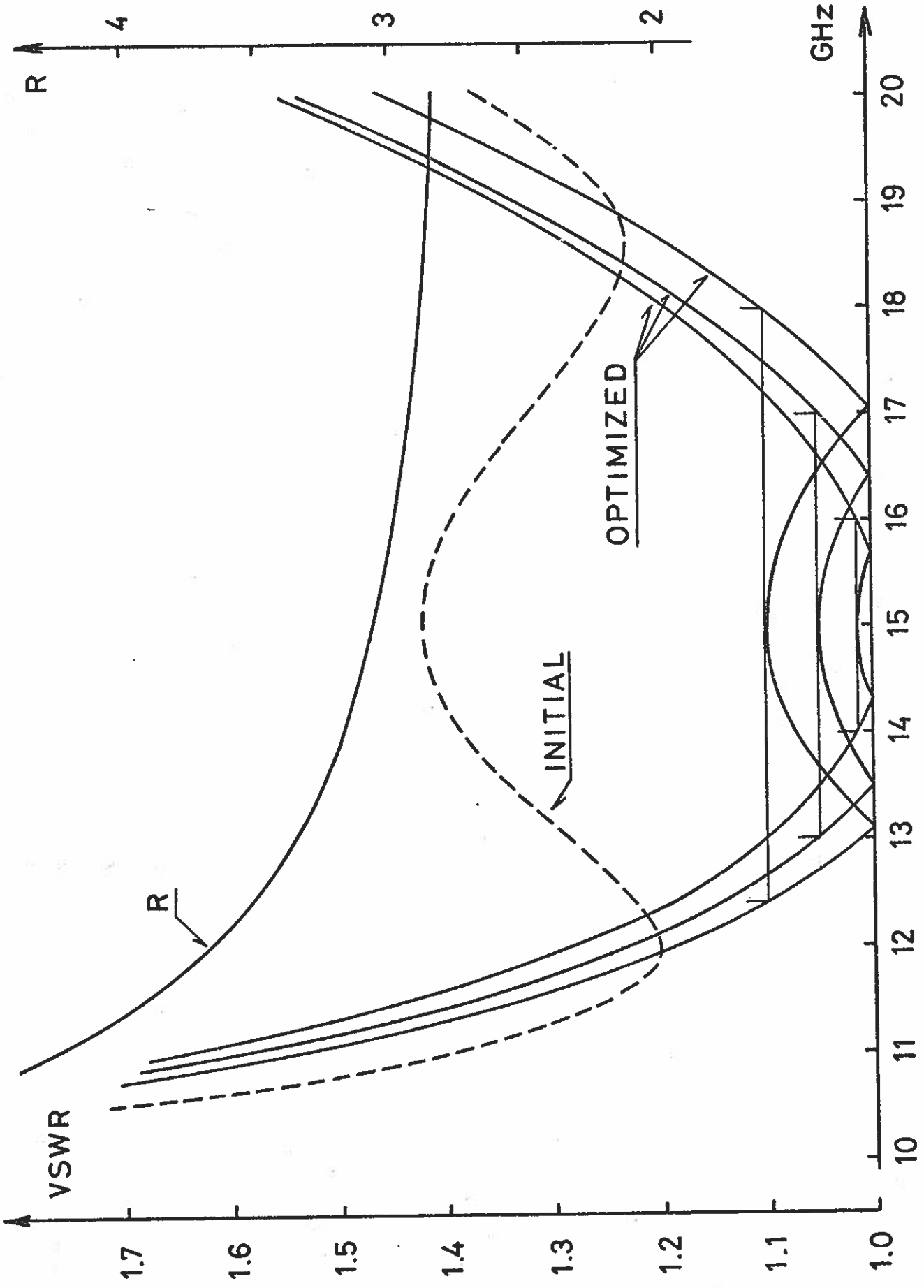

Fig. 9. Optimized ridge waveguide transformers with two sections.

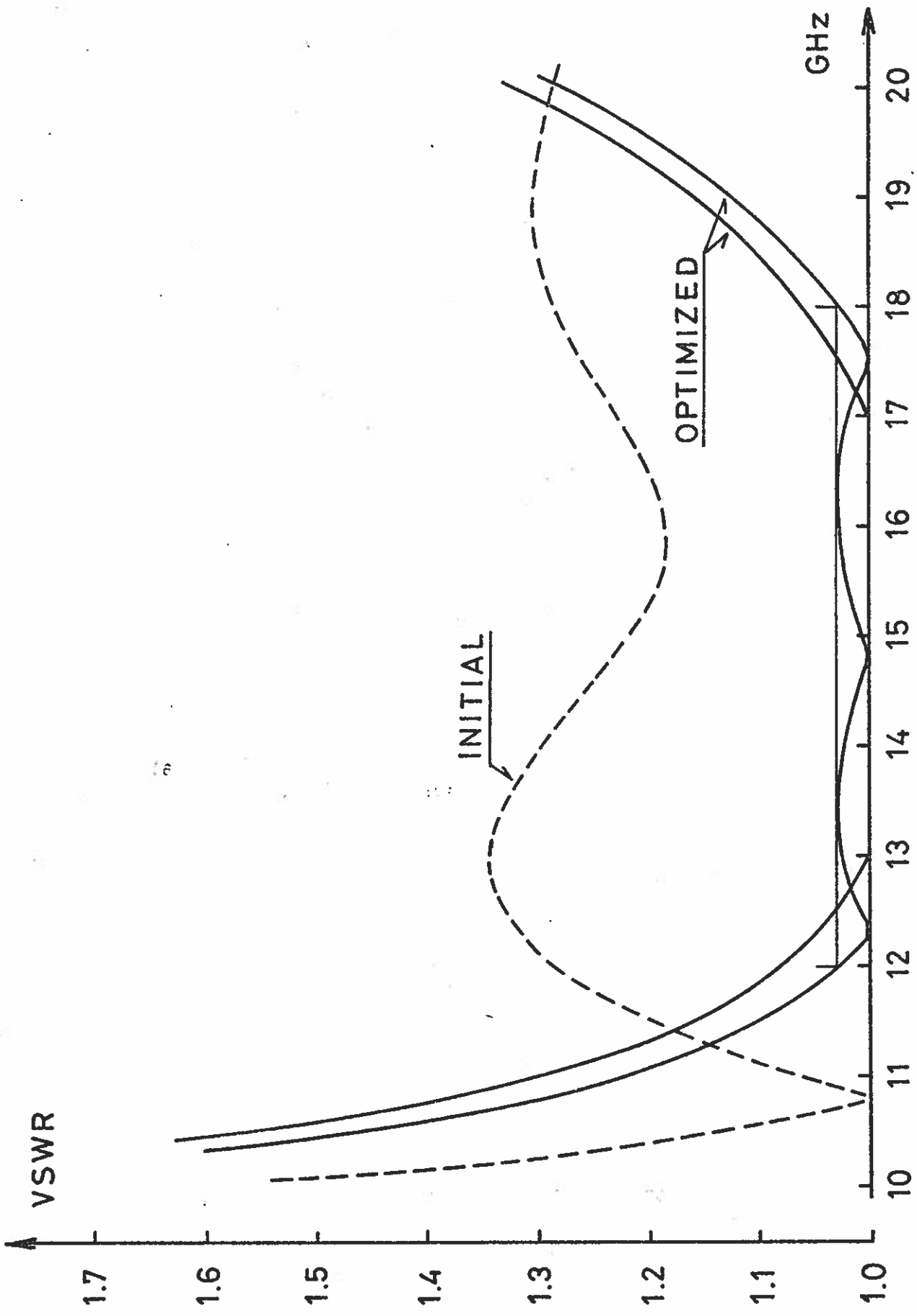

Fig. 10. Optimized ridge waveguide transformers with three sections.

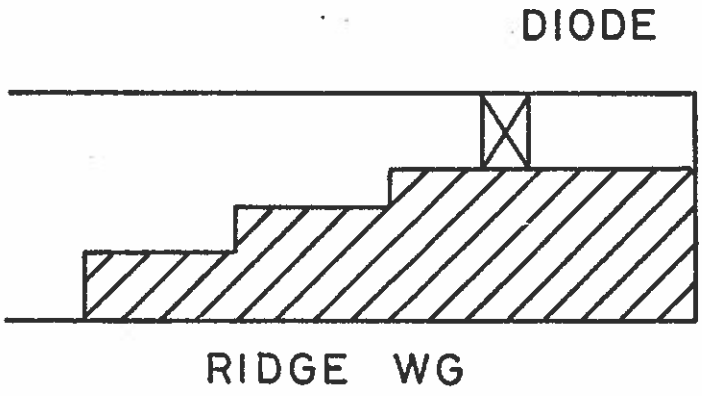

Fig. 11. Basic modulator structure.

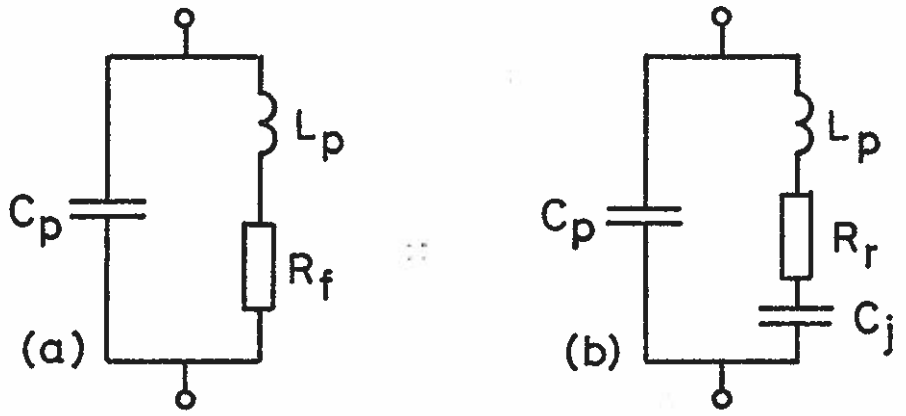

Fig. 12. Small signal equivalent circuits for PIN diode.
(a) Forward bias. (b) Reverse bias.

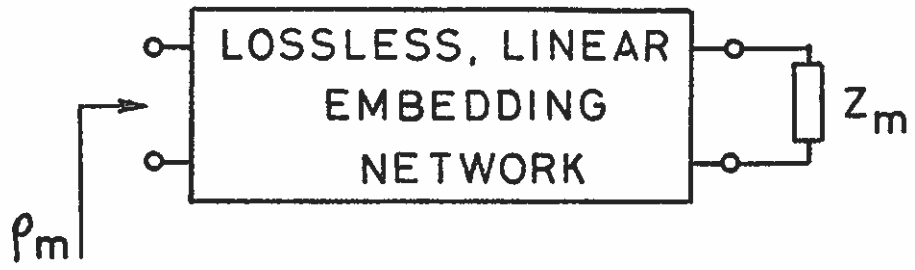

Fig. 13. Hyperbolic middle point impedance matching problem.

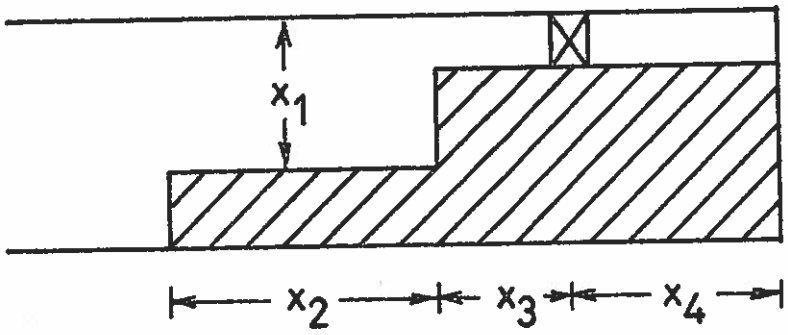

Fig. 14. Actual modulator structure with optimization parameters $\underline{x}$. a_1=15.8, b_1=7.9, a_2=7.0, and b_2=2.0 mm.

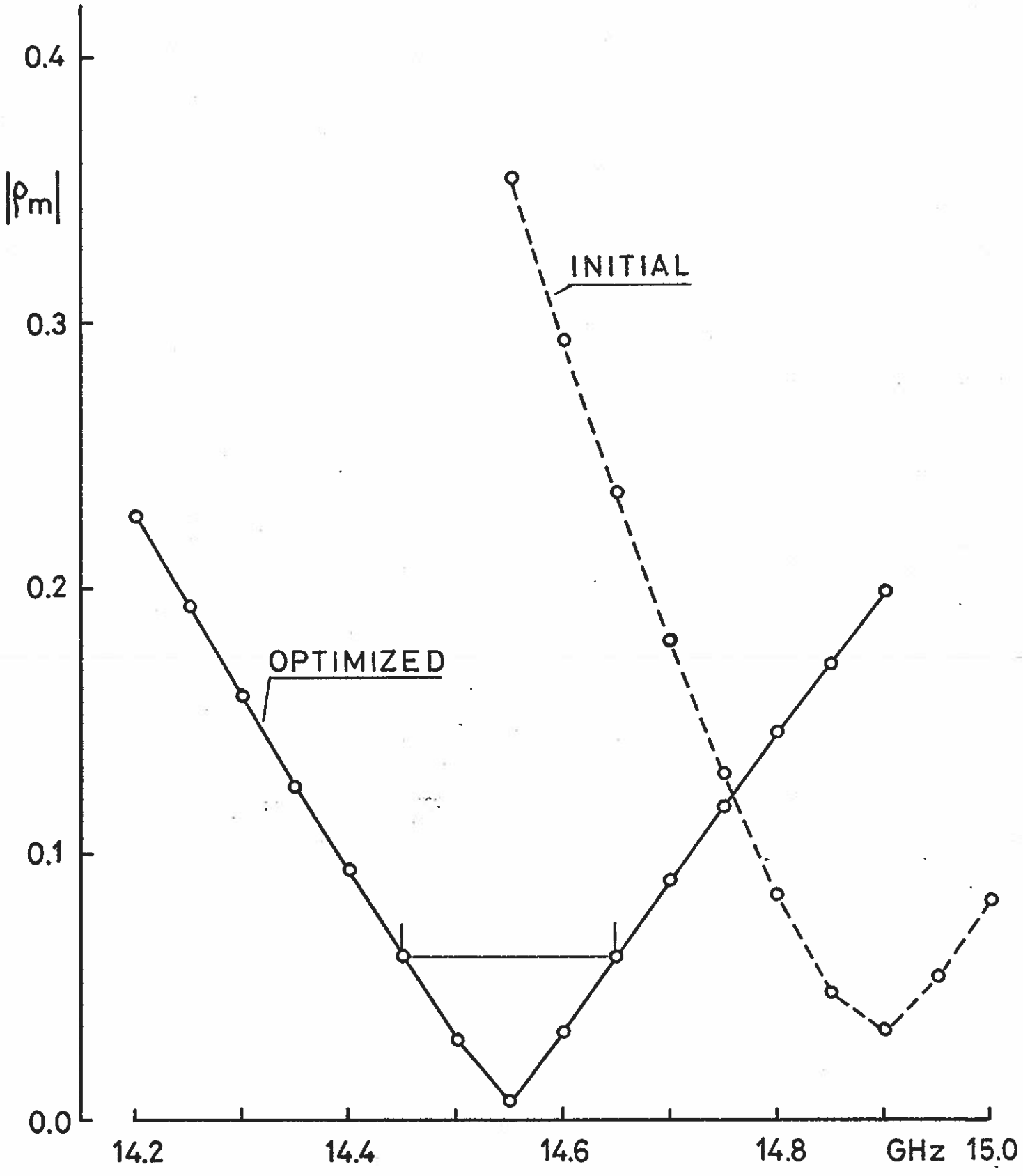

Fig. 15. Initial and optimized frequency responses for modulator.

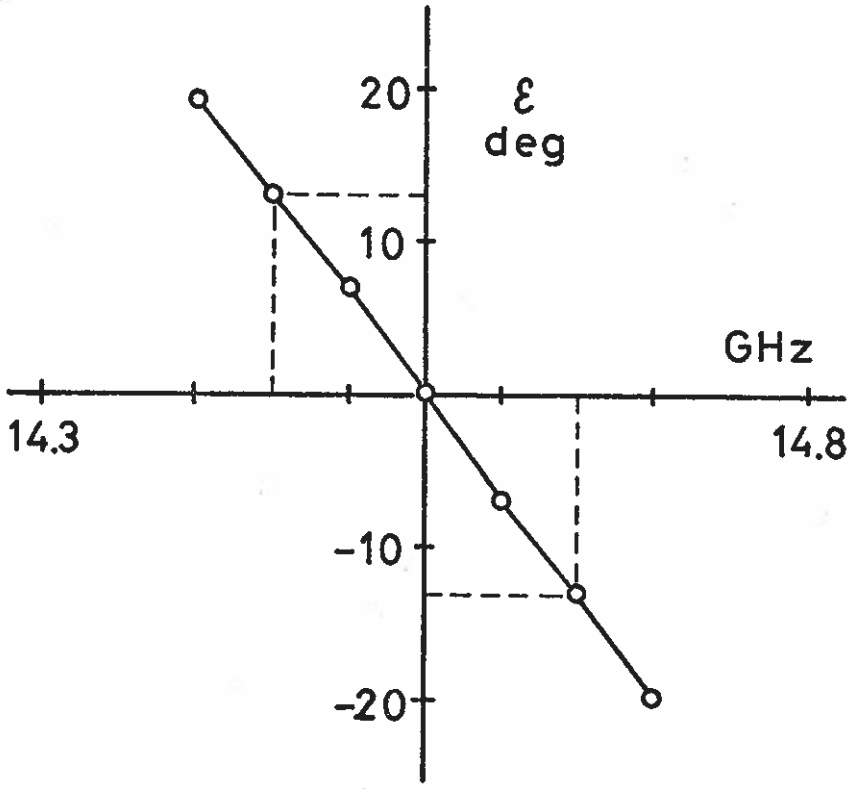

Fig. 16. Resulting phase error as function of frequency.